Applications of the Jaynes-Cummings model for the detection of nonorthogonal quantum states

M. Sasaki,[1,*] T. S. Usuda,[1] O. Hirota,[1] and A. S. Holevo[2]
[1]Research Center for Quantum Communications, Tamagawa University, Tokyo 194, Japan
[2]Steklov Mathematical Institute, Moscow, Russia

(Received 16 August 1995)

This paper presents two kinds of applications of the Jaynes-Cummings model to improve detection schemes for the binary phase-shift-keyed signals of the coherent states $|\alpha\rangle$ and $|-\alpha\rangle$. The first application raises the amount of exact retrodiction of a mixture made by choosing at random from $|\alpha\rangle$ and $|-\alpha\rangle$. The second application is concerned with realizing the optimum receiver to achieve a low decision error. Instead of optical detection, atomic level detection after mapping from them to two-level states of an atom will be proposed.

PACS number(s): 03.65.Bz, 42.50.−p

I. INTRODUCTION

How to differentiate between nonorthogonal states is a central issue in quantum communication science. Nonorthogonality of quantum states identified as information signals causes finite error probability in the detection process. Even if orthogonal states are transmitted as signals, they easily lose orthogonality under energy loss in the channel of communication systems. In almost all cases, the signal states are received as nonorthogonal ones. From a technological point of view, it is important to control received quantum states before detection in order to improve receiving performance. This idea is called the received quantum-state control [1,2].

In this paper we show some schemes of quantum state control based on the Jaynes-Cummings model (JCM). The JCM is the simplest mathematical description of the interaction between a single atom and a quantum field, such as an optical or microwave field, and has been studied extensively both theoretically and experimentally. Although many of these works are related to quantum-state preparation, for example, generation of the squeezed state, Schrödinger cat state, and so on, only a few works deal with the received quantum-state control. Here applications will be shown for two kinds of issues.

The first is the following: A mixture of quantum systems is prepared by choosing at random (with equal probability) from a set in state $|\phi_0\rangle$ and a set in $|\phi_1\rangle$. How many times can we exactly retrodict the state from the inspected signal sequences? We consider the total amount of exact state retrodictions or, equivalently, a fraction of its cases per each detection in the sequences. This has been discussed by Ivanovic [3] and Peres [4]. They showed an improved scheme achieving the maximum amount of exact retrodiction. This scheme is based on orthogonalization between the states $|\phi_0\rangle$ and $|\phi_1\rangle$ by the use of an interaction with an additional probe system. However, physical realizations have never been mentioned. We show how the JCM plays a role.

The second issue is concerned with the optimum decision process giving lower error probability when nonorthogonal quantum states $|\phi_0\rangle$ and $|\phi_1\rangle$ are transmitted. The states $|\phi_0\rangle$ and $|\phi_1\rangle$ are conditioned by hypotheses H_0 and H_1, respectively. At the receiver, the hypothesis is based on the measurement results. The lowest error limit known so far is the one given by Helstrom, which is now called Helstrom's bound. He showed a mathematical solution for the optimum decision [5]. After his work, the realization problem of the optimum decision process continues to be studied. Dolinar proposed a way of realizing this process [6]. It is a feedback measurement based on photon counting. Unfortunately, there is a difficulty in realizing it in an actual device, that is, immediate response to sending a feedback signal just after photon counting is required. A simpler and more practical method is desired for quantum communication. As the first step toward this goal, we shall present another view for the realization of Helstrom's bound. It is the mapping from the signal states $|\phi_0\rangle$ and $|\phi_1\rangle$ to other simpler states. A mapping scheme using the JCM is presented.

Here it is worth mentioning the relationship between these two issues. The first one can also be thought of as a decision problem. The decision error arises from the detection that fails the exact retrodiction. However, Ivanovic and Peres's scheme, which realizes the maximum amount of exact retrodiction, does not give the minimum error probability in binary decision. It is merely the optimization of the probability for orthogonalization between $|\phi_0\rangle$ and $|\phi_1\rangle$ to occur in the interaction between the signal and probe systems. The second issue is realizing the minimum error probability in binary decision.

II. EXACT RETRODICTION

A simple way for exact retrodiction is direct measurement to distinguish $|\phi_0\rangle$ from $|\bar{\phi}_0\rangle$, where $|\bar{\phi}_0\rangle$ is defined as $|\bar{\phi}_0\rangle\langle\bar{\phi}_0| = \hat{I} - |\phi_0\rangle\langle\phi_0|$ with unit operator $\hat{I}$. If $|\bar{\phi}_0\rangle$ is detected, we can be sure that the state is $|\phi_1\rangle$. If $|\phi_0\rangle$ is detected, there are still two possibilities: The state is $|\phi_0\rangle$ itself, or the state is $|\phi_1\rangle$ because of the finite overlap $\langle\phi_1|\phi_0\rangle$ $(\equiv\kappa)$. A fraction of cases of exact retrodiction is $\frac{1}{2}(1-\kappa^2)$ in this method.

Ivanovic [3] and Peres [4] showed that this amount can be raised by the following method. First, the signal system under investigation is correlated to a probe system by means of a unitary evolution in the extended space of the signal and

[*]Permanent address: Ayase LSI Research Center of NKK, Ayase 252, Japan.

probe systems. One then measures the probe that is in the specified state. The signal states are reduced by this measurement and result in orthogonal states under certain conditions. Let $\{|\phi_0\rangle, |\phi_1\rangle\}$ be projected onto a orthonormal set $\{|e_0\rangle, |e_1\rangle\}$ as

$$|\phi_0\rangle=\left(\frac{1+\kappa}{2}\right)^{1/2}|e_0\rangle+\left(\frac{1-\kappa}{2}\right)^{1/2}|e_1\rangle \tag{1a}$$

and

$$|\phi_1\rangle=\left(\frac{1+\kappa}{2}\right)^{1/2}|e_0\rangle-\left(\frac{1-\kappa}{2}\right)^{1/2}|e_1\rangle. \tag{1b}$$

And let $\{|\uparrow\rangle, |\downarrow\rangle\}$ be an orthonormal set for the probe system. Two-dimensional space is enough to be considered as the probe system. It will correspond to the upper- and lower-level states of a two-level atom in the example that is explained later. Peres pointed out that the unitary evolution required is a simple rotation in the subspace spanned by $\{|e_0\rangle |\downarrow\rangle, |e_1\rangle |\downarrow\rangle\}$. The unitary operator for this rotation can be expressed as

$$U(\theta)=\exp\ \theta(|e_0\rangle|\uparrow\rangle\langle\downarrow|\langle e_1|-|e_1\rangle|\downarrow\rangle\langle\uparrow|\langle e_0|). \tag{2}$$

Taking the input probe state as $|\uparrow\rangle$ and setting $\theta=\tan^{-1}\sqrt{2\kappa/(1-\kappa)}$, we see that the states are transformed into the following:

$$U(\theta)|\uparrow\rangle|\phi_0\rangle=\left(\frac{1-\kappa}{2}\right)^{1/2}|\uparrow\rangle(|e_0\rangle+|e_1\rangle)-\sqrt{\kappa}|\downarrow\rangle|e_1\rangle \tag{3a}$$

and

$$U(\theta)|\uparrow\rangle|\phi_1\rangle=\left(\frac{1-\kappa}{2}\right)^{1/2}|\uparrow\rangle(|e_0\rangle-|e_1\rangle)-\sqrt{\kappa}|\downarrow\rangle|e_1\rangle. \tag{3b}$$

As seen, if the probe state is found in $|\uparrow\rangle$, two signal states are always orthogonal, which can be distinguished unambiguously. The probability of this occurring is $1-\kappa$, which is greater than that in direct measurement $\frac{1}{2}(1-\kappa^2)$. Essential is the state reduction due to the probe measurement, which brings nonunitarity to the signal system. Such a state is often called *a posteriori state*. We adopt the terminology *a posteriori state method* for controlling the overlap between signal states by measuring the probe.

The question here is how to realize the unitary process of Eq. (2). Let signals be the binary coherent states $|\alpha\rangle$ and $|-\alpha\rangle$, which are commonly used in optical communication. The bases of the signal space $\{|e_0\rangle,|e_1\rangle\}$ are now

$$|e_0\rangle=\frac{1}{\sqrt{2(1+\kappa)}}(|\alpha\rangle+|-\alpha\rangle), \tag{4a}$$

$$|e_1\rangle=\frac{1}{\sqrt{2(1-\kappa)}}(|\alpha\rangle-|-\alpha\rangle). \tag{4b}$$

They are so-called even and odd coherent states [7]. What then is the process of Eq. (2), which is confined in the subspace spanned $\{|e_0\rangle|\uparrow\rangle,|e_1\rangle|\downarrow\rangle\}$? It is not so obvious. However, it is not necessary to make a process exactly the same as Eq. (2). Rather, only the final states, Eqs. (3a) and (3b), are required. In this direction, we demonstrate that the JCM plays a role very close to this purpose.

To begin, we briefly summarize *a posteriori state method* in terms of operator formalism. The Hamiltonian of the Jaynes-Cummings model is expressed as the following:

$$\begin{aligned}\hat{H}=&\hbar\omega\hat{a}^\dagger\hat{a}+\tfrac{1}{2}\hbar\nu(|\uparrow\rangle\langle\uparrow|-|\downarrow\rangle\langle\downarrow|)\\&+\hbar g(\hat{a}^\dagger|\downarrow\rangle\langle\uparrow|+\hat{a}|\uparrow\rangle\langle\downarrow|),\end{aligned} \tag{5}$$

where $\hat{a}$ ($\hat{a}^\dagger$) is an annihilation (creation) operator for a single-mode optical field with the angular frequency ω; $|\uparrow\rangle$ and $|\downarrow\rangle$ have the meaning of the upper- and lower-level states, respectively; and ν is the angular frequency corresponding to the atomic level separation. The coupling constant g between the optical field and the atom is taken to be real. The initial states of signal and probe systems are assumed to be $|\alpha\rangle_F$ and $|\sigma\rangle_A$ ($\sigma=\uparrow$ or $\downarrow$), respectively. Hereafter the indices F and A for the states are used to represent signal field and atomic probe, respectively, for the sake of clarity. Let $\mathscr{H}_F$ and $\mathscr{H}_A$ be the Hilbert spaces for the signal and probe systems, respectively. The unitarity for the whole space $\mathscr{H}_F\otimes\mathscr{H}_A$ is an essential requirement for real physical processes. The unitary evolution operator on the extended space is $\hat{U}^{(F\otimes A)}=\exp(-i\hat{H}t/\hbar)$. The state of the whole system after the interaction is expressed as

$$|\psi_{\rm out}\rangle_{F\otimes A}=\hat{U}^{(F\otimes A)}|\alpha\rangle_F|\sigma\rangle_A. \tag{6}$$

One measures atomic state by the atomic level detector [8]. If the atomic state is specified as $|\sigma'\rangle_A$, then the signal state reduces to the state

$$\begin{aligned}|\phi_{\rm out}\rangle_F&=\left(\frac{1}{\sqrt{c}}\right)\ {}_A\langle\sigma'|\psi_{\rm out}\rangle_{F\otimes A}\\&=\left(\frac{1}{\sqrt{c}}\right)\ {}_A\langle\sigma'|\hat{U}^{(F\otimes A)}|\sigma\rangle_A|\alpha\rangle_F\\&=\left(\frac{1}{\sqrt{c}}\right)\ \hat{t}(\sigma'|\sigma)|\alpha\rangle_F,\end{aligned} \tag{7}$$

where c is an appropriate normalization constant and

$$\hat{t}(\sigma'|\sigma)\equiv{}_A\langle\sigma'|\hat{U}^{(F\otimes A)}|\sigma\rangle_A. \tag{8}$$

It is easy to see that this normalization constant c is the probability that the transition from $|\sigma\rangle_A$ to $|\sigma'\rangle_A$ will occur in the probe system, under the initial state $|\alpha\rangle_F$ of the signal system. Therefore we denote it as $P(\sigma'|\sigma;\alpha)$:

$$P(\sigma'|\sigma;\alpha)\equiv{}_F\langle\alpha|\hat{t}^\dagger(\sigma'|\sigma)\hat{t}(\sigma'|\sigma)|\alpha\rangle_F. \tag{9}$$

Then we can express a transition in the signal system by an operator when the probe system is found in the state $|\sigma'\rangle_A$ after the measurement. That is, by defining

$$\hat{T}(\sigma'|\sigma;\alpha)=\frac{1}{\sqrt{P(\sigma'|\sigma;\alpha)}}\hat{t}(\sigma'|\sigma), \tag{10}$$

the transition is described by

$$|\phi_{\mathrm{out}}(\sigma'|\sigma;\alpha)\rangle_F=\hat{T}(\sigma'|\sigma;\alpha)|\alpha\rangle_F, \tag{11}$$

where the symbol "$(\sigma'|\sigma;\alpha)$" is added to the output state in order to show explicitly that this state is created by an observation of the transition "$|\sigma\rangle_A\rightarrow|\sigma'\rangle_A$" in the probe system. We emphasize that the $\hat{T}(\sigma'|\sigma;\alpha)$ is in general a nonunitary operator and includes a transition probability in the probe system under the given initial signal state $|\alpha\rangle_F$. The unitarity for the whole space $\mathscr{H}_F\otimes\mathscr{H}_A$ is expressed as

$$1=\sum_{\sigma} P(\sigma'|\sigma;\alpha)\hat{T}^{\dagger}(\sigma'|\sigma;\alpha)\hat{T}(\sigma'|\sigma;\alpha). \tag{12}$$

The operator $\hat{T}(\sigma'|\sigma;\alpha)$ is called the conditional isometric operator in quantum information science [9,10]. The probability related to the process caused by this operator is conditioned by each signal state. It might be a natural expression for *quantum channel* in a communication system.

Now we discuss the behavior of the overlap between signal states $|\alpha\rangle$ and $|-\alpha\rangle$ in the resonant JCM with $\omega=\nu$. We take the initial probe state as $|\uparrow\rangle$; $\hat{t}(\uparrow|\uparrow)$ and $\hat{t}(\downarrow|\uparrow)$ are expressed as

$$\hat{t}(\uparrow|\uparrow)\equiv\sum_{n=0}^{\infty} \exp[-i(n+\tfrac{1}{2})\omega t]\cos(gt\sqrt{n+1})|n\rangle\langle n| \tag{13a}$$

and

$$\hat{t}(\downarrow|\downarrow)\equiv-i\sum_{n=0}^{\infty} \exp[-i(n+\tfrac{1}{2})\omega t]\times\sin(gt\sqrt{n+1})|n+1\rangle\langle n|, \tag{13b}$$

where the state $|n\rangle$ is the photon-number eigenstate of the signal field. The probabilities of the atomic transitions $|\uparrow\rangle$ to $|\uparrow\rangle$ and $|\uparrow\rangle$ to $|\downarrow\rangle$ are

$$P(\uparrow|\uparrow;\alpha)=\exp(-|\alpha|^2)\sum_{n=0}^{\infty} \cos^2(gt\sqrt{n+1}) \frac{|\alpha|^{2n}}{n!} \tag{14a}$$

and

$$P(\downarrow|\uparrow;\alpha)=\exp(-|\alpha|^2)\sum_{n=0}^{\infty} \sin^2(gt\sqrt{n+1}) \frac{|\alpha|^{2n}}{n!}. \tag{14b}$$

Note that $P(\sigma|\uparrow;\alpha)=P(\sigma|\uparrow;-\alpha)$, $(\sigma=\uparrow,\downarrow)$. The overlap after the interaction is

$$K(\uparrow)\equiv\langle-\alpha|\hat{T}'(\uparrow|\uparrow;-\alpha)\hat{T}(\uparrow|\uparrow;\alpha)|\alpha\rangle =\frac{1}{P(\uparrow|\uparrow;\alpha)}e^{-|\alpha|^2}\left\{\sum_{n=\mathrm{even}} \cos^2(gt\sqrt{n+1}) \frac{|\alpha|^{2n}}{n!} -\sum_{n=\mathrm{odd}} \cos^2(gt\sqrt{n+1}) \frac{|\alpha|^{2n}}{n!}\right\} \tag{15a}$$

or

$$K(\downarrow)\equiv\langle-\alpha|\hat{T}^{\dagger}(\downarrow|\uparrow;-\alpha)\hat{T}(\downarrow|\uparrow;\alpha)|\alpha\rangle =\frac{1}{P(\downarrow|\uparrow;\alpha)}e^{-|\alpha|^2}\left\{\sum_{n=\mathrm{even}} \sin^2(gt\sqrt{n+1}) \frac{|\alpha|^{2n}}{n!} -\sum_{n=\mathrm{odd}} \sin^2(gt\sqrt{n+1}) \frac{|\alpha|^{2n}}{n!}\right\}, \tag{15b}$$

depending on which state of the probe atom is detected, $|\uparrow\rangle$ or $|\downarrow\rangle$, respectively. Orthogonalization of the signal states, that is, $K(\uparrow)=0$, or $K(\downarrow)=0$, occurs at the interaction parameters gt, which satisfy

$$\sum_{n=\mathrm{even}} \cos^2(gt\sqrt{n+1}) \frac{|a|^{2n}}{n!}=\sum_{n=\mathrm{odd}} \cos^2(gt\sqrt{n+1}) \frac{|\alpha|^{2n}}{n!}, \tag{16a}$$

$$\sum_{n=\mathrm{even}} \sin^2(gt\sqrt{n+1}) \frac{|\alpha|^{2n}}{n!}=\sum_{n=\mathrm{odd}} \sin^2(gt\sqrt{n+1}) \frac{|\alpha|^{2n}}{n!}, \tag{16b}$$

respectively. Let us set the parameter gt to satisfy Eq. (16a). Then the exact retrodiction is possible when the atom is detected as $|\uparrow\rangle$, giving $K(\uparrow)=0$. We want a fraction of those cases,

$$P(\uparrow|\uparrow;\alpha)=2\sum_{n=\mathrm{even}} \cos^2(gt\sqrt{n+1}) \frac{|\alpha|^{2n}}{n!}, \tag{17}$$

to be as large as possible.

A numerical example of the case $\alpha=1$ is shown in Fig. 1. Figure 1(a) shows the behaviors of $K(\uparrow)$ and $K(\downarrow)$, varying the interaction parameter gt. The solid and dotted lines represent $K(\uparrow)$ and $K(\downarrow)$, respectively. The horizontal one-dotted line shows the inner product without the interaction, $\langle-\alpha|\alpha\rangle$. It can be seen that the signal states are orthogonalized at certain parameters gt where $K(\uparrow)$ or $K(\downarrow)$ crosses over the gt axis. Figure 1(b) shows the behaviors of $P(\uparrow|\uparrow;\alpha)$ (solid line) and $P(\downarrow|\uparrow;\alpha)$ (dotted line). Those kinds of state evolution in the JCM do not exactly correspond to the one in Eqs. (3a) and (3b). In the JCM, the signal state whose initial state is $|\alpha\rangle$ or $|-\alpha\rangle$ may run over the infinite dimensional space spanned by the Fock states $\{|n\rangle;n=1,2,\ldots\}$, while the unitary evolution described by Eq. (2) is confined in the two-dimensional subspace of the signal and probe states. The optimum amount of exact retrodiction predicted by Ivanovic and Peres's method for the case of $\alpha=1$ is about $1-\kappa=0.864\,67$. In our scheme with the JCM, it is not obvious how to pick up the interaction parameter gt for realizing the same value. A closer value obtained in the range of $0<gt<20$ is about 0.834 176 at $gt=15.687\,8$ as $P(\uparrow|\uparrow;\alpha)$ when $|\uparrow\rangle$ is specified. The behaviors expanded around this point, indicated by the arrow, is presented in Fig. 2. The definition of lines are the same as in Fig. 1. It is an absolute requirement that the number of $P(\uparrow|\uparrow;\alpha)$ should be less than the value $1-\kappa$. The larger Hilbert space cannot make the probability of orthogonalization any larger.

It is worth mentioning that their behaviors obey the unitarity condition

$$\langle-\alpha|\alpha\rangle=P(\uparrow|\uparrow;\alpha)K(\uparrow)+P(\downarrow|\uparrow;\alpha)K(\downarrow). \tag{18}$$

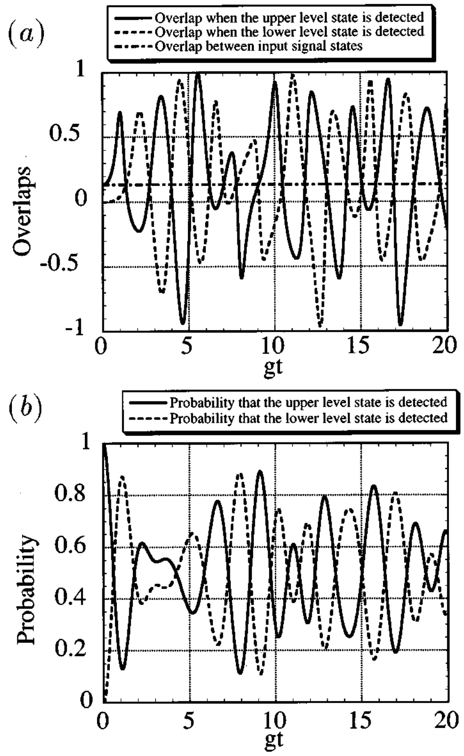

FIG. 1. A numerical example of the received quantum-state control with the resonant Jaynes-Cummings model in the case of $\alpha=1$. (a) The overlaps $K(\uparrow)$ and $K(\downarrow)$ varying the interaction parameter gt, which is dimensionless. (b) The probabilities of the atomic transitions. The solid and dotted lines correspond to the atomic transition channels $|\uparrow\rangle$ to $|\uparrow\rangle$ and $|\uparrow\rangle$ to $|\downarrow\rangle$, respectively. The horizontal one-dotted line in (a) shows the initial value of the overlap $\langle -\alpha|\alpha\rangle$.

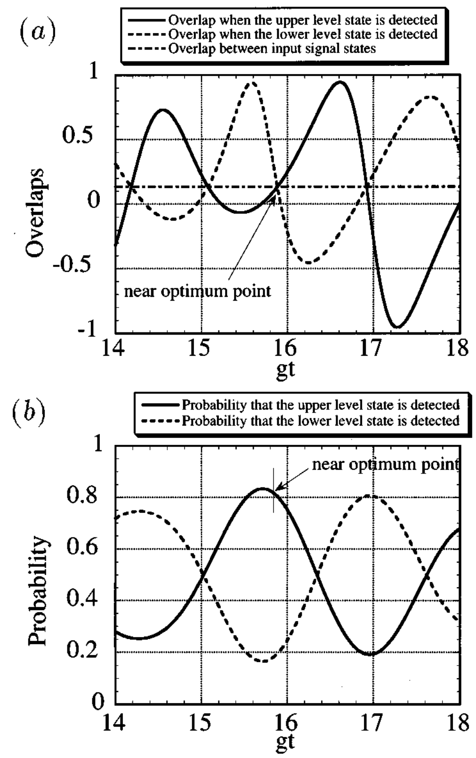

FIG. 2. The behaviors in Fig. 1 are magnified around the near optimum point, indicated by the arrow. The probability of orthogonalization closest to the theoretical maximum $1-\kappa=0.864\,67$, in the range of $0<gt<20$, is about 0.834176 at $gt=15.687\,8$ as $P(\uparrow|\uparrow;\alpha)$ when $|\uparrow\rangle$ is specified.

Usuda discussed the details about them [11]. This relation prevents the inner products $K(\uparrow)$ and $K(\downarrow)$ to be orthogonalized for the same interaction parameter.

III. OPTIMUM DECISION PROCESS

Let us move to the second issue. The optimum decision process derived by Helstrom is expressed in terms of the probability operator measure (POM) [12–17], which is defined as a non-negative Hermitian operator satisfying the resolution of identity,

$$\hat{\Pi}_i=\hat{\Pi}_i^{\dagger}\geqslant 0 \quad (i=0,1), \tag{19a}$$

$$\hat{\Pi}_0+\hat{\Pi}_1=\hat{I}, \tag{19b}$$

where $\hat{I}$ is a unit operator of the two-dimensional signal space. For the case of linearly independent signals, they can be written in the form of orthogonal spectral measure (Kennedy's lemma [18]):

$$\hat{\Pi}_0=|\omega_0\rangle\langle\omega_0|, \tag{20a}$$

$$\hat{\Pi}_1=|\omega_1\rangle\langle\omega_1|, \tag{20b}$$

where $\{|\omega_0\rangle,|\omega_1\rangle\}$ is a complete orthonormal set of the signal space to which $|\phi_0\rangle$ and $|\phi_1\rangle$ belong. Therefore, the decision process is mathematically described as merely a projection to the basis $\{|\omega_0\rangle,|\omega_1\rangle\}$. The error probability in the optimum decision process becomes

$$\begin{aligned} P_e(\mathrm{opt}) &= \xi|\langle\omega_1|\phi_0\rangle|^2+(1-\xi)|\langle\omega_0|\phi_1\rangle|^2 \\ &= \tfrac{1}{2}\left[1-\sqrt{1-4\xi(1-\xi)|\langle\phi_1|\phi_0\rangle|^2}\right], \end{aligned} \tag{21}$$

where ξ and $1-\xi$ are prior probabilities for the signal states $|\phi_0\rangle$ and $|\phi_1\rangle$, respectively.

Now let us consider the optimum decision for a particular case of the binary coherent signals $|\alpha\rangle$ and $|-\alpha\rangle$ with the same a priori probabilities, i.e., $\xi=\frac{1}{2}$. The channel model is depicted in Fig. 3. The solid lines represent correct decision channels, while the dotted lines represent error channels. The concrete expressions for $|\omega_0\rangle$ and $|\omega_1\rangle$ were derived by Osaki and Hirota [19] as

$$|\omega_0\rangle=\left(\frac{1+\sqrt{1-\kappa^2}}{2(1-\kappa^2)}\right)^{1/2}|\alpha\rangle-\left(\frac{1-\sqrt{1-\kappa^2}}{2(1-\kappa^2)}\right)^{1/2}|-\alpha\rangle \tag{22a}$$

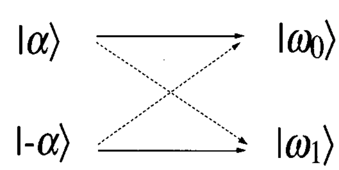

FIG. 3. Channel model for the optimum decision process. The solid lines represent correct decision channels, the dotted lines error channels.

and

$$|\omega_1\rangle = \left(\frac{1-\sqrt{1-\kappa^2}}{2(1-\kappa^2)}\right)^{1/2}|\alpha\rangle - \left(\frac{1+\sqrt{1-\kappa^2}}{2(1-\kappa^2)}\right)^{1/2}|-\alpha\rangle, \tag{22b}$$

where $\kappa = \langle\alpha|-\alpha\rangle = \exp(-2|\alpha|^2)$. They are the so-called Schrödinger cat states made of the signal states $|\alpha\rangle$ and $|-\alpha\rangle$. (Ban, Osaki, and Hirota recently provided a systematic derivation method of the decision operator $\hat{\Pi}_i$ for the general case of n dimensional signals being linearly independent [20]. The method consists of orthogonalization of the signal states and unitary transformation from these orthogonal bases to appropriate bases. It is instructive to understand the structure of the optimum decision process). The optimum decision in this case is equivalent to *alternative observation* of these two kinds of Schrödinger cat states. The error probability is

$$P_e(\text{opt}) = \tfrac{1}{2}(1-\sqrt{1-\kappa^2}). \tag{23}$$

In Dolinar's method, this process is realized by a kind of stochastic treatment, i.e., feedback measurement depending on the photon-counting results. However, we wish to find a more systematic design theory of the receiver realizing the optimum decision process. For this purpose, it might be beneficial to decompose the optimum decision process, if any, into the ones with clear physical correspondence.

As an example, we show that the alternative observation of the states $|\omega_0\rangle$ and $|\omega_1\rangle$ can be mapped into binary detection of two-level states of an atom. The mapping process is mainly composed of two steps, each of which is constructed with unitary evolutions.

The first step is a generation of even and odd coherent states by use of the nonresonant atom-optical field interaction. This generation scheme was originally proposed by Brune *et al.* [21] and Haroche [22]. It can be described by a unitary evolution operator $\hat{U}_1$ in the extended space of the optical signal field and the atom. That is, after receiving the signal state—let it be $|\alpha\rangle$ for clarity—it is correlated with an atomic superposition state $1/\sqrt{2}(|\uparrow\rangle+|\downarrow\rangle)$ via $\hat{U}_1$. The output state is fully entangled as

$$\hat{U}_1 \frac{1}{\sqrt{2}}(|\uparrow\rangle+|\downarrow\rangle)|\alpha\rangle = \left(\frac{1+\kappa}{2}\right)^{1/2}|\uparrow\rangle|\alpha_+\rangle + \left(\frac{1-\kappa}{2}\right)^{1/2}|\downarrow\rangle|\alpha_-\rangle, \tag{24a}$$

where

$$|\alpha_\pm\rangle = \frac{1}{\sqrt{2(1\pm\kappa)}}(|\alpha e^{-i(\pi/2)}\rangle \pm |\alpha e^{i(\pi/2)}\rangle). \tag{24b}$$

The states $|\alpha_\pm\rangle$ are the even and odd coherent states. The details on $\hat{U}_1$ will be explained in the Appendix.

The second step is a rotation in tensor space spanned by composite basis $|\uparrow\rangle|\alpha_+\rangle$ and $|\downarrow\rangle|\alpha_-\rangle$. An evolution operator is

$$\hat{U}_2 = \exp\frac{\pi}{4}(|\uparrow\rangle|\alpha_+\rangle\langle\alpha_-|\langle\downarrow| - |\downarrow\rangle|\alpha_-\rangle\langle\alpha_+|\langle\uparrow|). \tag{25}$$

The final state is the following:

$$|\psi(\alpha)\rangle = \hat{U}_2\hat{U}_1\frac{1}{\sqrt{2}}(|\uparrow\rangle+|\downarrow\rangle)|\alpha\rangle = \frac{\sqrt{1+\kappa}+\sqrt{1-\kappa}}{2}|\uparrow\rangle|\alpha_+\rangle - \frac{\sqrt{1+\kappa}-\sqrt{1-\kappa}}{2}|\downarrow\rangle|\alpha_-\rangle. \tag{26}$$

When the received signal is $|-\alpha\rangle$, the final state is

$$|\psi(-\alpha)\rangle = \hat{U}_2\hat{U}_1\frac{1}{\sqrt{2}}(|\uparrow\rangle+|\downarrow\rangle)|-\alpha\rangle = \frac{\sqrt{1+\kappa}-\sqrt{1-\kappa}}{2}|\uparrow\rangle|\alpha_+\rangle - \frac{\sqrt{1+\kappa}+\sqrt{1-\kappa}}{2}|\downarrow\rangle|\alpha_-\rangle. \tag{27}$$

In detection, only measurement of the atom is made by the level detector. The optical field components are not concerned. Therefore, the states reduce to the following mixed states, by tracing out the optical field components:

$$\hat{\rho}_A(\alpha) = \mathrm{Tr}_F[|\psi(\alpha)\rangle\langle\psi(\alpha)|] = \frac{1+\sqrt{1-\kappa^2}}{2}|\uparrow\rangle\langle\uparrow| + \frac{1-\sqrt{1-\kappa^2}}{2}|\downarrow\rangle\langle\downarrow|, \tag{28a}$$

$$\hat{\rho}_A(-\alpha) = \mathrm{Tr}_F[|\psi(-\alpha)\rangle\langle\psi(-\alpha)|] = \frac{1-\sqrt{1-\kappa^2}}{2}|\uparrow\rangle\langle\uparrow| + \frac{1+\sqrt{1-\kappa^2}}{2}|\downarrow\rangle\langle\downarrow|. \tag{28b}$$

They are the mapped states. The processes are schematically summarized in Fig. 4. Thus the binary decision of the signal states $|\alpha\rangle$ and $|-\alpha\rangle$ with the decision operators $\hat{\Pi}_0 = |\omega_0\rangle\langle\omega_0|$ and $\hat{\Pi}_1 = |\omega_1\rangle\langle\omega_1|$ can be mapped into the atomic states $\hat{\rho}_A(\alpha)$ and $\hat{\rho}_A(-\alpha)$ with the decision operators $\hat{\Pi}_0^m = |\uparrow\rangle\langle\uparrow|$ and $\hat{\Pi}_1^m = |\downarrow\rangle\langle\downarrow|$, respectively. The channel model is shown in Fig. 5. The error probability is written as

$$P_e(\text{opt}) = \tfrac{1}{2}\langle\downarrow|\hat{\rho}_A(\alpha)|\downarrow\rangle + \tfrac{1}{2}\langle\uparrow|\hat{\rho}_A(-\alpha)|\uparrow\rangle = \tfrac{1}{2}(1-\sqrt{1-\kappa^2}). \tag{29}$$

The first step of the mapping process can be realized by a current technique in the cavity QED, as explained in the Appendix. However, physical correspondence to the second

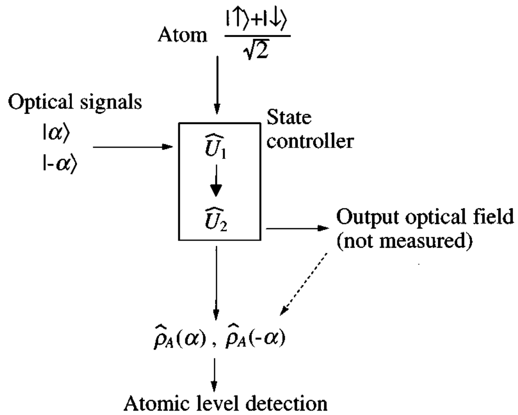

FIG. 4. The mapping process. It is mainly composed of two steps, each of which is described by the unitary operator $\hat{U}_1$ and $\hat{U}_2$. After these interactions, only measurement of the atom is made by the atomic level detector.

step is not yet clear. The state evolution in the second step is exactly the same as the one for the Ivanovic and Peres scheme to realize the optimum amount of exact retrodiction as discussed in Sec. II [see Eqs. (2) and (25)]. As shown there, the state control with the resonant JCM can achieve the amount of exact retrodiction to a closer value to the optimum point. But how to realize exactly the state evolution of Eq. (2) or (25), a rotation of the composite basis, is a remaining problem. Required are further studies of how much closer one can come to the result of that rotation by use of the JCM.

IV. SUMMARY

Two kinds of applications of the JCM to the received quantum state control were presented. The first application is concerned with the exact retrodiction of an ensemble of two nonorthogonal states. It was shown that the state control with the resonant JCM can achieve the amount of the retrodiction close to the optimum value, which can theoretically be possible in the Ivanovic and Peres scheme.

The second application is the realization of Helstrom's receiver, which gives the lowest decision error to date for nonorthogonal quantum state signals. The mapping scheme from binary coherent state signals $|\alpha\rangle$ and $|-\alpha\rangle$ to two-level atomic states $|\uparrow\rangle$ and $|\downarrow\rangle$ was proposed. It enables us to replace the complicated optical measurement required in Helstrom's receiver with the simple atomic level detection. It was shown that the mapping process can be described by unitary process. We decomposed it into two steps. The first step is the generation of the Schrödinger cat states of optical coherent field with the nonresonant regime of the JCM. The second step is the rotation in the two-dimensional subspace spanned by the composite basis of the optical Schrödinger cat state and the atomic state, whose physical realization needs to be studied further.

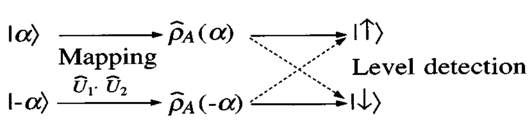

FIG. 5. Channel model for our mapping scheme. After the mapping, detection is made only for the atomic states being mixed. The solid lines represent correct decision channels, the dotted lines error channels.

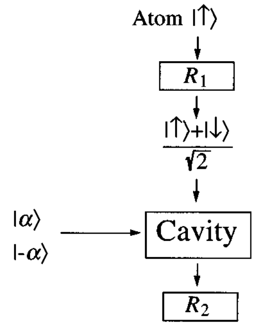

FIG. 6. Experimental setup for generation of the even and odd coherent states. A cavity is located between two Ramsey zones, R_1 and R_2, where injected atoms are irradiated by a high-intensity laser beam. An atomic beam prepared in the upper-level state crosses successively zone R_1, the cavity, and zone R_2. At zone R_1, the superposition state is produced. At the cavity, it interacts with the signal coherent field, generating the entangled state. After passage of the atom through zone R_2, another entangled state is made, whose optical field components are the even and odd coherent states.

ACKNOWLEDGMENTS

The authors wish to thank Dr. M. Ban (Advanced Research Lab. of Hitach), Dr. K. Yamazaki, and Dr. M. Osaki for their helpful discussions.

APPENDIX: GENERATION OF THE EVEN AND ODD COHERENT STATES

The generation scheme of the even and odd coherent states, proposed by Brune *et al.* [21] and Haroche [22], was applied to the mapping process in Sec. III. Its physical description is given here. Figure 6 is an experimental setup. A cavity is located between two Ramsey zones, R_1 and R_2, where injected atoms are irradiated by a high-intensity laser beam. An atomic beam prepared in the upper-level state crosses successively zone R_1, the cavity, and zone R_2. The beam is adjusted in such a way that only a single atom exists inside the cavity, and this single atom interacts with the coherent field as the received signal state.

At the first zone, the atomic state is transformed from the upper-level state to a superposition of the upper- and lower-level states by pumping with the laser beam, which can be treated as a classical field for the atom. It can be described by the semiclassical JCM, derived by replacing the operator $g\hat{a}$ with the c number $\epsilon e^{-i\nu\tau}$, where τ is the interacting period, in Eq. (5). The driving field $\epsilon e^{-i\nu\tau}$ is resonant with the atomic transition. The Hamiltonian is

$$\hat{H}_R = \tfrac{1}{2}\hbar\nu(|\uparrow\rangle\langle\uparrow| - |\downarrow\rangle\langle\downarrow|) + \hbar(\epsilon e^{-i\nu\tau}|\uparrow\rangle\langle\downarrow| + \epsilon^* e^{i\nu\tau}|\downarrow\rangle\langle\uparrow|). \tag{A1}$$

By choosing the phase of ϵ as $\epsilon = i|\epsilon|$ and setting $|\epsilon|\tau = \pi/4$ and $\nu\tau = \pi$, the evolution of the atomic state is described by the operator $\hat{U}_R$ as

$$\hat{U}_R|\uparrow\rangle = -i\,\frac{|\uparrow\rangle + |\downarrow\rangle}{\sqrt{2}}. \tag{A2}$$

This atomic superposition state enters the cavity to interact with the signal field, assumed to be $|\alpha\rangle$ for clarity. The interaction is in the nonresonant regime; that is, the detuning $\delta = \nu - \omega \gg g$ in the JCM [Eq. (5)]. The effective Hamiltonian is

$$\hat{H}_C = \hbar\omega\hat{n} + \tfrac{1}{2}\hbar(\nu + g_{\mathrm{eff}})(|\uparrow\rangle\langle\uparrow| - |\downarrow\rangle\langle\downarrow|) + \hbar g_{\mathrm{eff}}(|\uparrow\rangle\langle\uparrow| - |\downarrow\rangle\langle\downarrow|)\hat{n}, \tag{A3}$$

where $g_{\mathrm{eff}} = g^2/\delta$ and $\hat{n}$ is the photon-number operator for the signal field. Let t be the interaction period in the cavity. By adjusting $\nu t = \frac{3}{2}\pi$ and $g_{\mathrm{eff}}t = \pi/2$, the state evolution in the cavity is described by the operator $\hat{U}_C$ as

$$\hat{U}_C|\alpha\rangle\hat{U}_R|\uparrow\rangle = \frac{i}{\sqrt{2}}\,(|\uparrow\rangle|\alpha e^{-i\omega t}e^{-i(\pi/2)}\rangle + |\downarrow\rangle|\alpha e^{-i\omega t}e^{i(\pi/2)}\rangle). \tag{A4}$$

The atom exits the cavity and enters the second zone R_2, whose effect is the same as the first one. Further operation of $\hat{U}_C$ to the state of Eq. (A4) leads to the following state:

$$\hat{U}_R\hat{U}_C|\alpha\rangle\hat{U}_R|\uparrow\rangle = \tfrac{1}{2}|\uparrow\rangle(|\alpha e^{-i\omega t}e^{-i(\pi/2)}\rangle + |\alpha e^{-i\omega t}e^{i(\pi/2)}\rangle) + \tfrac{1}{2}|\downarrow\rangle(|\alpha e^{-i\omega t}e^{-i(\pi/2)}\rangle - |\alpha e^{-i\omega t}e^{i(\pi/2)}\rangle), \tag{A5}$$

which is equivalent to the state of Eqs. (24a) and (24b). The operator $\hat{U}_1$ in Sec. III corresponds to $-i\hat{U}_R\hat{U}_C$.

[1] O. Hirota, O. Kagami, and M. Takahara, Trans. Inst. Electron. In. Commun. Eng. Jpn. **E70**, 801 (1987).
[2] O. Hirota, Opt. Commun. **67**, 204 (1988).
[3] I. D. Ivanovic, Phys. Lett. A **123**, 257 (1987).
[4] A. Peres, Phys. Lett. A **128**, 19 (1988).
[5] C. W. Helstrom, *Quantum Detection and Estimation Theory* (Academic, New York, 1976).
[6] S. J. Dolinar, Research Laboratory of Electronics, MIT, Quarterly Progress Report No. 111, 1973 (unpublished).
[7] I. A. Malkin and V. I. Man'ko, *Dynamical Symmetries and Coherent States of Quantum Systems* (Nauka, Moscow, 1979).
[8] G. Rempe, F. Schmidt-Kaler, and H. Walther, Phys. Rev. Lett. **64**, 2783 (1990).
[9] O. Hirota, Phys. Lett. A **155**, 343 (1991).
[10] O. Hirota, *Open System & Information Dynamics* (N. Copernicus University Press, Toruń, 1994), Vol. 2, No. 2, p. 157.
[11] T. S. Usuda, Inst. Electron. Inf. Commun. Eng. Jpn. Technical Report OPE94-123, 1995 (unpublished).
[12] H. P. Yuen, R. S. Kennedy, and M. Lax, IEEE Trans. Inf. Theory **21**, 125 (1975).
[13] V. P. Belavkin and R. L. Stratonovich, Radio Eng. Electron. Phys. (USSR) **18**, 1839 (1973).
[14] E. Davies, *Quantum Theory of Open Systems* (Academic, London, 1976).
[15] A. S. Holevo, *Probabilistics and Statistical Aspects of Quantum Theory* (North-Holland, Amsterdam, 1982).
[16] M. Ozawa, J. Math. Phys. **34**, 5596 (1993).
[17] O. Hirota and S. Ikehara, Trans. Inst. Electron. Inf. Commun. Eng. Jpn. **E65**, 627 (1977).
[18] R. S. Kennedy, Research Laboratory of Electronics, MIT, Quarterly Progress Report No. 110, 1973 (unpublished).
[19] M. Osaki and O. Hirota, *Quantum Communication and Measurement* (Plenum, New York, 1995), p. 401.
[20] M. Ban, M. Osaki, and O. Hirota, IEEE Trans. Inf. Theory (to be published).
[21] M. Brune, S. Haroche, V. Lefevre, J. M. Raimond, and N. Zagury, Phys. Rev. Lett. **65**, 976 (1990).
[22] S. Haroche, *Fundamental Systems in Quantum Optics* (North-Holland, Amsterdam, 1992), pp. 768–940, and references therein.